AIP | Applied Physics Letters

Compressive-tensile deformation of nanocrystalline nickel at high pressure and temperature conditions

Xiaohui Yu, Yuejian Wang, Jianzhong Zhang, Hongwu Xu, and Yusheng Zhao

Citation: Appl. Phys. Lett. **103**, 043118 (2013); doi: 10.1063/1.4816744
View online: http://dx.doi.org/10.1063/1.4816744
View Table of Contents: http://apl.aip.org/resource/1/APPLAB/v103/i4
Published by the AIP Publishing LLC.

Compressive-tensile deformation of nanocrystalline nickel at high pressure and temperature conditions

Xiaohui Yu,[1,2,a)] Yuejian Wang,[3] Jianzhong Zhang,[2] Hongwu Xu,[2,4] and Yusheng Zhao[5,a)]
[1]*Beijing National Laboratory for Condensed Matter Physics and Institute of Physics, Chinese Academy of Sciences, Beijing 100190, China*
[2]*LANSCE Division, Los Alamos National Laboratory, Los Alamos, New Mexico 87545, USA*
[3]*Department of Physics, Oakland University, Rochester, Michigan 48309, USA*
[4]*EES Division, Los Alamos National Laboratory, Los Alamos, New Mexico 87545, USA*
[5]*HiPSEC and Department of Physics and Astronomy, University of Nevada, Las Vegas, Nevada 89154, USA*

(Received 17 April 2013; accepted 8 July 2013; published online 25 July 2013)

We conducted uniaxial compressive and tensile deformation on nanocrystalline Ni at a confining pressure of 6 GPa and temperatures up to 900 °C. The determined compressive yield strength is 0.8 GPa, identical to the tensile yield strength obtained in the same deformation experiment, indicating that the Bauschinger effect is absent in nanocrystalline Ni. The yield strength obtained at 6 GPa is also comparable to that at ambient pressure, suggesting that the dislocation-mediated mechanisms are no longer activated during plastic deformation. Based on peak intensity and peak width analyses, grain rotation and grain growth are main factors underlying the plastic deformation. © *2013 AIP Publishing LLC*. [http://dx.doi.org/10.1063/1.4816744]

In coarse-grained metals, plastic deformation is mainly achieved by dislocation motion in crystal grains and interaction with preexisting microstructure (other defects, grain boundaries, etc.). During plastic deformation in these materials, dislocations accumulate at grain boundaries, which give rise to work hardening. When the grain size is reduced to the nano-scale, a few to 100 nm, nanocrystalline materials exhibit a rich variety of interesting and novel behavior due to the influence of a large volume fraction of atoms at grain boundaries. The mechanical properties such as yield and flow stresses, for example, increase with the inverse square root of the grain size in the range of tens of nanometers to micrometers, which is the well known Hall-Petch relation.[1,2] Below a critical grain size of 40 nm, the strength in some metals and alloys increases with increasing grain size, a phenomenon that is commonly referred as an inverse or anomalous Hall–Petch relation.[3–5] Over the last decade, both experimental[6–13] and theoretical[14–19] studies have been devoted to revealing the deformation mechanisms for nanocrystalline materials. It has been suggested that at a critical grain size, 20 to 40 nm for fcc metals, grain boundary sliding and migration become the dominant deformation mechanisms because the stress to bow out dislocations approaches the theoretical shear stress.[20–22] Such deformation mechanisms are not accessible to their coarse-grained counterparts and have rendered nanocrystalline materials unique mechanical properties such as high strength and diminishing work-hardening.

Recently, high-pressure compressive deformation has been investigated on nanocrystalline Ni,[23] which exhibits substantially high yield strength of 2.3 GPa and significant work hardening. However, the experiments were performed under triaxial loading and hence are unable to quantify the uniaxial stress in the sample. As a result, the constitutive strain-stress relation under confined high pressure is still unknown. To fully understand the promise and potential of nanocrystalline materials, we conducted experiments on nano Ni at confined high pressure using *in situ* synchrotron X-ray diffraction (XRD) coupled with a deformation-DIA.[24] The, thus, obtained data are of fundamental importance not only for the comprehensive understanding of nano-mechanics but also for optimal design of desired properties.[25,26]

The nano-Ni powders were prepared by mechanical ball milling. The as-prepared sample has a grain-size distribution of 8–12 nm and a very high dislocation density of $\sim 10^{16}\,m^{-2}$.[27] The uniaxial deformation experiment at high pressure was performed on the 13-BM-D beamline at the GSECARS sector of the Advanced Photon Source, Argonne National Laboratory, using the deformation-DIA (D-DIA).[24] For deformation under confined high pressure, the two vertical anvils in D-DIA can be driven independently to introduce compressive or tensile uniaxial strains. Differential stress was produced in the specimen with hard alumina pistons placed on the two ends of the specimen. The sample was separated from the alumina pistons by gold foils, which were used as strain markers for measuring the sample length or total strain. Using this system, we carried out deformation experiments on a fully dense nano Ni cylinder at a confining pressure of 6 GPa and temperatures up to 900 °C.

The two-dimensional diffraction patterns were collected by an X-ray sensitive CCD camera (Fig. 1(a)), which provide full Debye-Scherrer rings. By moving the aperture slits out of the beam and exposing an X-ray fluorescent screen viewed by another CCD camera (Fig. 1(b)), X-ray radiograph of the sample was recorded alternating with the diffraction. The macroscopic or total strain was determined from the radiographs by the relation, $\varepsilon_{true} = (l_0 - l)/l_0$, where l is the sample length under a given deformation condition and l_0 is the sample length at the reference point, normally, the starting point of deformation.

The theory used to describe elastic lattice stress in the D-DIA system is the same as that in the uniaxial diamond-anvil

a)Authors to whom correspondence should be addressed. Electronic addresses: yuxh-jl@hotmail.com and yusheng.zhao@unlv.edu

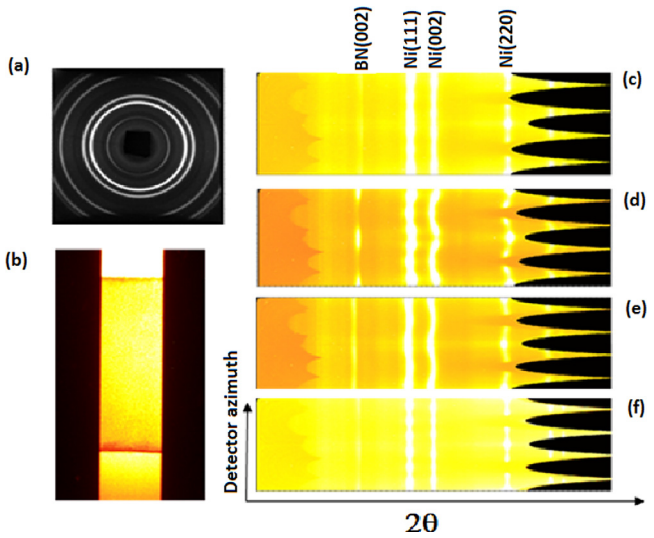

FIG. 1. (a) A typical CCD image recording diffraction Debye rings. (b) An example of x-ray radiographic image for sample length measurement. (c)–(f) Representative X-ray diffraction patterns by plotting 2θ (horizontal axis) versus azimuth angle (vertical axis). Deviation from a straight line is a measure of lattice strain. (c), (d), and (f) correspond to the starting point of deformation cycle, 9% true strain, and restoration to 1% true strain, respectively, all at a confining pressure of 6 GPa; (f) is collected after heating to 900 °C at the end of the tensile deformation.

cell (DAC) experiments.[28,29] More detailed discussion about the differential stress calculation is shown in Ref. 30.

Figures 1(a) and 1(b) show typical examples of diffraction Debye rings and x-ray radiographic image of the sample recorded at a confining pressure of 6 GPa, which is defined as the starting point of the deformation. Figures 1(c)–1(f) are the representative XRD patterns converted from the original 2D diffraction pattern (Fig. 1(a)) in polar coordinates into Cartesian systems. In Figure 1(c), the diffraction line positions exhibit no azimuthal dependence, indicating a stress-free state at the starting point of deformation. Figures 1(d) and 1(e) are patterns collected, respectively, at 9% true strain of the shortening cycle, the largest deformation point of the experiment, and after retraction to 1% of the deformation. As clearly shown in both graphs, the position of each diffraction line varies with the detector azimuth. The 2θ maxima at azimuth angles of 0° and 180° in Figure 1(d) correspond to the direction of the compressive principle stress σ_1, with $\sigma_1 > \sigma_3$, under which the sample undergoes axial shortening. The 2θ minima at azimuth angles of 0° and 180° in Figure 1(e) correspond to the condition of $\sigma_1 < \sigma_3$, under which the sample undergoes tensile deformation. In Figure 1(f), the stress is relaxed because the sample was heated to 900 °C.

Figure 2(a) shows the strain-stress relations derived from the reflection planes of (111) and (200) at 6 GPa and room temperature. Both curves follow similar trends of variation during the entire course of deformation. In particular, in the linear portion of the deformation, the two curves essentially overlap with each other. We define the stress at the starting points of deviation from the linear relation as the yield strength. In the compression stage, the sample yields at ~1.4% true strain with a corresponding yield stress of 0.8 GPa, which is substantially smaller than our previous determination.[23] The yield strength in this paper is considered to be more accurate because the sample is deformed in

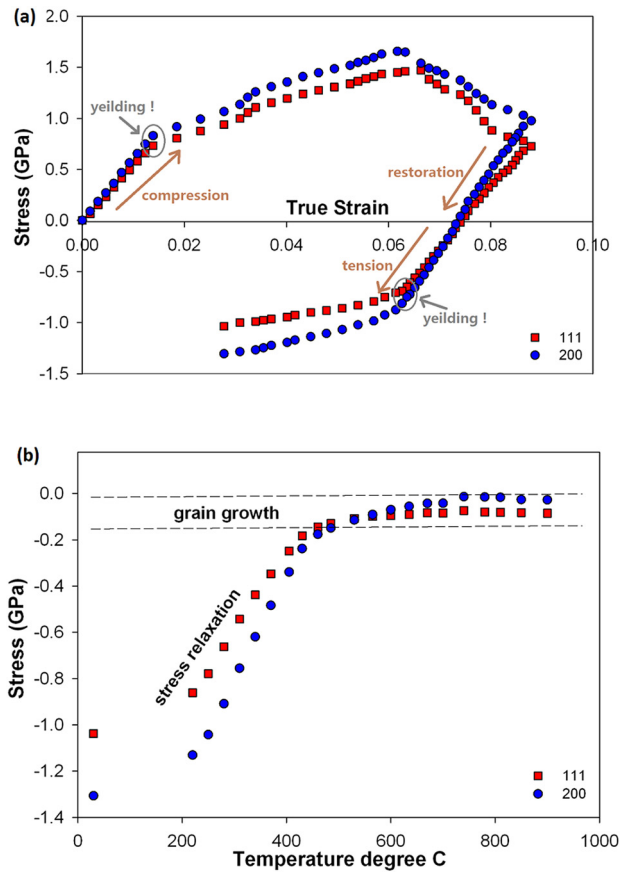

FIG. 2. (a) True strain-stress curve at room temperature, (b) heating from 30 °C to 900 °C. The strain rate is around 6.03×10^{-6}.

an uniaxial experiment with well-defined stress states, whereas in Ref. 23, the experiment was conducted under triaxial loading and is hence unable to derive the classic stress-strain curve. To further understand the plastic deformation of nano Ni, we deformed the sample to a large strain of ~9%. During the restoration stage, the differential stress returns to zero when the macroscopic strain in the sample recovers from 8.8% to 7.5%. After reaching the zero-stress point, the restoration enters the tension mode although the sample length is still less than the original point. At 6.2% macroscopic strain or 1.3% tensile strain, the nano Ni sample reaches the tensile yield point with yield strength of ~0.8 GPa. This value is comparable to the tensile yield stress of 0.82 ~ 0.85 GPa reported for 20 nm Ni but it is 50% higher than that of coarse-grained Ni (0.55 GPa at ambient conditions).[31]

The fact that the tensile yield strength is the same as compressive yield strength during the deformation indicates that the Bauschinger effect is absent in nanocrystalline Ni. For coarse grained metals, the yield strength typically decreases when the direction of plastic strain is reversed during the deformation. This so-called Bauschinger effect is generally associated with the dislocation structure, dislocation movement history, and the interaction between dislocations and grain boundaries. The absence of the Bauschinger effect in nanocrystalline Ni indicates that the dislocations are not active during the compressive-tensile deformation. To take this argument one step further, the nano Ni at the yield points of both compressive and tensile deformation should

have the same dislocation structures as in the starting sample.

It is well known that for coarse-grained metals the confining pressure tends to increase the strength and ductility. For potassium of micron grain size,[32] the pressure-dependent yield strength can well be described by the equation

$$\sigma_0 = \sigma_{00}[1 + (C_0'/C_0)P],$$

where σ_{00} is the yield strength at ambient pressure, σ_0 is the strength at pressure P, C_0' is the pressure derivative of the effective elastic constant, and P is the superimposed confining pressure. There are a number of studies on bulk metals[32–35] at different confining pressures using both theoretical and experimental methods. Kleipeis *et al.*,[33] for example, observed a linear increase of yield strength with pressure in polycrystalline vanadium powders and foils up to 40 GPa. In some metals such as U and Ta, the yield strength could increase by as much as ten times when the confining pressure increases. Such pressure-induced strengthening is due to the fact that the shear modulus G increases with increasing pressure, resulting in larger stress fields around dislocations. Thus, the application of pressure can effectively hinder dislocation movement and increase the yield stresses. In contrast, our experimental data on nano Ni show that the yield strength at a confining pressure of 6 GPa is comparable to that at ambient pressure,[31] suggesting that the dislocation-mediated processes are no longer activated during the deformation. Similar conclusions have also been reached from the reversible peak broadening observed in nanocrystalline Fe[36] and nanocrystalline Ni[21,23] and (100% in nano-Fe and 84%–100% in nano-Ni) during stress loading/unloading. Thus far, all experimental data seem to indicate that dislocations in nanocrystalline Ni are fasten inside the grains and no additional dislocations are generated during the plastic deformation when grain size is below a critical length scale.

At the end of the deformation cycles, we increased temperature to 900 °C to study thermal effect on the stress state (Fig. 2(b)). When temperature increases from 30 °C to 420 °C, nanocrystalline Ni releases nearly 90% of the stress, from 1.3 GPa to 0.2 GPa, indicating substantial stress relaxation at high temperature. When temperature is further increased from 420 °C to 900 °C, the stress changes slightly from 0.2 GPa to 0, a behavior that is similar to our previous observations and is attributed to a relaxation mechanism dominated by grain growth.[23]

Figure 3 plots the variation of intensity ratio of I(111)/I(200) as a function of true strain, which shows remarkable correlations with the strain-stress curve of Figure 2. First, all kink points, namely, O, A, B, C, D, and E in Fig. 3, occur at the true strains that are essentially identical to those in the strain-stress curve. Second, in the elastic regimes of both compressive and tensile deformation, the intensity ratios remain unchanged (O-A and D-E in Fig. 3(a)). Most importantly, when nanocrystalline Ni starts to yield or deform plastically, the intensity ratios during both compressive and tensile cycles increase progressively with the microscopic strains (A-C and E-F in Fig. 3(a)), suggesting that the crystal reorientation, most likely in the form of grain rotation, is a dominating mechanism underlying the plastic deformation!

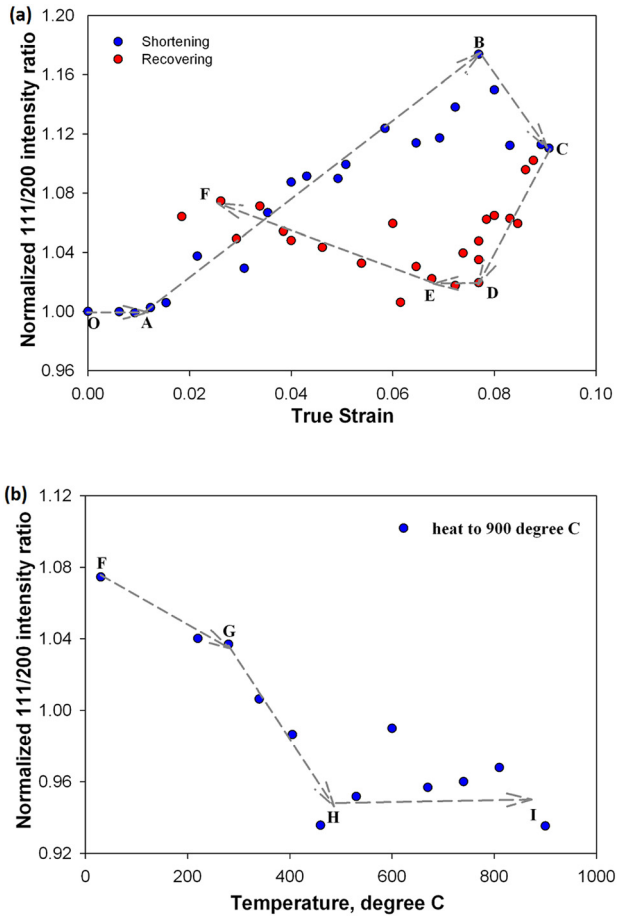

FIG. 3. (a) Normalized intensity (area) ratio I(111)/I(200) during the deformation at room temperature and (b) at the heating stage from 30 °C to 900 °C.

This deformation induced grain rotation was also observed by Wang *et al.*[37] using TEM on nano Ni. Inspection of Figures 2(b) and 3(b) also reveals correlations between thermally induced stress and peak intensity variations. Notably, the grain rotation dominates the stress relaxation at temperatures of 30–420 °C, whereas the intensity ratios remain unchanged at the grain-growth stage.

Interestedly, the stress in Fig. 2(a) decreases when the strain increases from 6% to 9%, showing a softening phenomenon, which is rarely observed in tensile tests on metals. In order to find physical mechanisms for this, we examine the peak width variations during the deformation, which is shown in Fig. 4. The (111) and (200) planes have very similar trends of variation with strain; so for clarity, only the (200) data are shown in this paper. A notable feature in Fig. 4 is the dramatic drop in peak width when the strain increases from 6.3% to 9% (BC), which correlates with the stress softening in Fig. 2(a) during the compressive deformation. It is known that the peak width is affected by the instrument factors, differential stress, dislocations and grain size.[23,38,39] As discussed above, the dislocations should not affect the deformation behavior of the nano Ni sample. Thus, the primary factor that contributes to the abnormal peak-width sharpening should be grain growth during the deformation, which, according to the Hall–Petch relation, would lead to the stress softening. Such strain-induced grain growth in nano materials has also been observed in previous studies.[40,41]

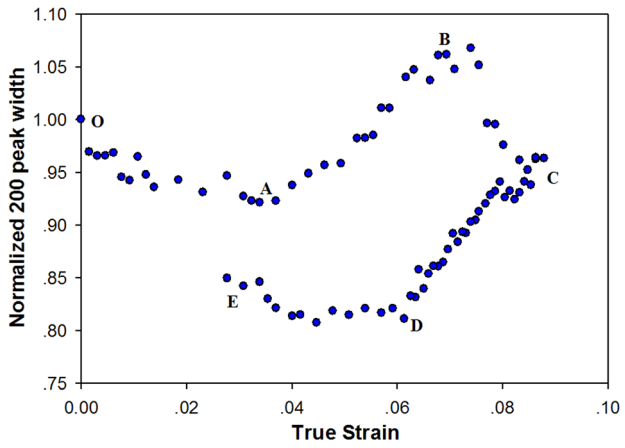

FIG. 4. Normalized FWHM for the (200) plane during the deformation at room temperature.

In summary, we conducted uniaxial deformation experiments using DIA on nanocrystalline Ni at the confining pressure of 6 GPa and temperatures up to 900 °C. From the measured strain-stress relations, we found that the Bauschinger effect is absent in nano Ni. In addition, the confining pressure does not seem to affect the yield strength of nano Ni, indicating that dislocations, although in a very high density, are no longer active during the plastic deformation. The peak intensity and peak width variations show good correlation with the strain-stress curves, suggesting that crystal reorientation, most likely in the form of grain rotation, and grain growth are dominating mechanisms underlying the plastic deformation.

This research was supported by Los Alamos National Laboratory, which is operated by Los Alamos National Security LLC under DOE Contract No. DE-AC52-06NA25396. The experimental work was carried out at beam line 13-BM-D at the Advanced Photon Source, Argonne National Laboratory.

[1]E. O. Hall, Proc. Phys. Soc. London, Sect. B **64**, 747 (1951).
[2]N. J. Petch, J. Iron Steel Inst., London **174**, 25 (1953).
[3]P. G. Sanders, J. A. Eastman, and J. R. Weertman, Acta Mater. **45**, 4019 (1997).
[4]J. Schiøtz and K. W. Jacobsen, Science **301**, 1357 (2003).
[5]L. Lu, X. Chen, X. Huang, and K. Lu, Science **323**, 607 (2009).
[6]M. A. Meyers, A. Mishara, and D. J. Bension, Prog. Mater. Sci. **51**, 427 (2006).
[7]F. D. Torre, H. V. Swygenhoven, and M. Victoria, Acta Mater. **50**, 3957 (2002).
[8]K. M. Youssef, R. O. Scattergood, K. L. Murty, and C. C. Koch, Appl. Phys. Lett. **85**, 929 (2004).
[9]H. Li and F. Ebrahimi, Appl. Phys. Lett. **84**, 4307 (2004).
[10]R. Schwaiger, B. Moser, M. Dao, N. Chollacoop, and S. Suresh, Acta Mater. **51**, 5159 (2003).
[11]S. Cheng, E. Ma, Y. Wang, L. J. Kecskes, K. M. Youssef, C. C. Koch, U. P. Trociewitz, and K. Han, Acta Mater. **53**, 1521 (2005).
[12]F. Ebrahimi, Z. Ahmed, and H. Li, Appl. Phys. Lett. **85**, 3749 (2004).
[13]C. A. Schuh, T. G. Nieh, and H. Iwasaki, Acta Mater. **51**, 431 (2003).
[14]J. Schiøtz, F. D. DiTolla, and K. W. Jacobsen, Nature **391**, 561 (1998).
[15]H. Van Swygenhoven and P. M. Derlet, Phys. Rev. B **64**, 224105 (2001).
[16]X. Li, Y. Wei, L. Lu, K. Lu, and H. Gao, Nature **464**, 877 (2010).
[17]V. Yamakov, D. Wolf, S. R. Phillpot, A. K. Mukherjee, and H. Gleiter, Nature Mater. **3**, 43 (2004).
[18]A. G. Frøseth, P. M. Derlet, and H. Van Swygenhoven, Scripta Mater. **54**, 477 (2006).
[19]H. Conrad and J. Narayan, Appl. Phys. Lett. **81**, 2241 (2002).
[20]H. Van Swygenhoven, Science **296**, 66 (2002).
[21]Z. Budrovic, H. Van Swygenhoven, P. M. Derlet, S. Van Petegem, and B. Schmitt, Science **304**, 273 (2004).
[22]Z. W. Shan, E. A. Stach, J. M. K. Wiezorek, J. A. Knapp, D. M. Follstaedt, and S. X. Mao, Science **305**, 654 (2004).
[23]Y. Zhao, J. Zhang, B. Clausen, T. Shen, G. T. Gray, and L. Wang, Nano Lett. **7**, 426 (2007).
[24]Y. Wang, W. B. Durham, I. C. Getting, and D. J. Weidner, Rev. Sci. Instrum. **74**, 3002 (2003).
[25]Y. S. Ko, T. Tsurumi, O. Fukunaga, and T. Yano, J. Mater. Sci. **36**, 469 (2001).
[26]Y. Zhao, J. Qian, L. L. Daemen, C. Pantea, J. Zhang, G. A. Voronin, and T. W. Zerda, Appl. Phys. Lett. **84**, 1356 (2004).
[27]T. Shen, J. Zhang, and Y. Zhao, Acta Mater. **56**, 3663 (2008).
[28]T. Uchida, N. Funamori, and T. Yagi, J. Appl. Phys. **80**, 739 (1996).
[29]S. Merkel, H. R. Wenk, J. Shu, G. Shen, P. Gillet, H. K. Mao, and R. J. Hemley, J. Geophys. Res. **107**, 2271, doi:10.1029/2001JB000920 (2002).
[30]See supplementary material at http://dx.doi.org/10.1063/1.4816744 for differential stress calculation.
[31]S. Cheng, J. Xie, A. D. Stoica, X. L. Wang, J. A. Horton, D. W. Brown, H. Choo, and P. K. Liaw, Acta Mater. **57**, 1272 (2009).
[32]J. O. Chua and A. L. Ruoff, J. Appl. Phys. **46**, 4659 (1975).
[33]J. P. Kleperis, H. Cynn, W. J. Evans, R. E. Rudd, L. H. Yang, H. P. Liermann and W. Yang, Phys. Rev. B **81**, 134107 (2010).
[34]S. T. Weir, J. Akella, C. Ruddle, T. Goodwin, and L. Hsiung, Phys. Rev. B **58**, 11258 (1998).
[35]P. D. Wu, J. D. Embury, D. J. Lloyd, Y. Huang, and K. W. Neale, Int. J. Plast. **25**, 1711 (2009).
[36]X. Yu, J. Zhang, L. Wang, Z. Ding, C. Jin, and Y. Zhao, Acta Mater. **59**, 3384 (2011).
[37]Y. B. Wang, B. Q. Li, M. L. Sui, and S. X. Mao, Appl. Phys. Lett. **92**, 011903 (2008).
[38]Y. Wang, J. Zhang, and Y. Zhao, Nano Lett. **7**, 3196 (2007).
[39]X. Yu, J. Zhang, Y. Zhang, L. Wang, and Y. Zhao, J. Appl. Phys. **111**, 113506 (2012).
[40]G. J. Fan, Y. D. Wang, L. F. Fu, H. Choo, P. K. Liaw, Y. Ren, and N. D. Browning, Appl. Phys. Lett. **88**, 171914 (2006).
[41]J. Monk and D. Farkas, Phys. Rev. B **75**, 045414 (2007).